JCI The Journal of Clinical Investigation

Tumor-infiltrating myeloid cells induce tumor cell resistance to cytotoxic T cells in mice

Tangying Lu, … , Michael B. Sporn, Dmitry Gabrilovich

J Clin Invest. 2011;121(10):4015-4029. https://doi.org/10.1172/JCI45862.

Research Article **Immunology**

Cancer immunotherapeutic approaches induce tumor-specific immune responses, in particular CTL responses, in many patients treated. However, such approaches are clinically beneficial to only a few patients. We set out to investigate one possible explanation for the failure of CTLs to eliminate tumors, specifically, the concept that this failure is not dependent on inhibition of T cell function. In a previous study, we found that in mice, myeloid-derived suppressor cells (MDSCs) are a source of the free radical peroxynitrite (PNT). Here, we show that pre-treatment of mouse and human tumor cells with PNT or with MDSCs inhibits binding of processed peptides to tumor cell–associated MHC, and as a result, tumor cells become resistant to antigen-specific CTLs. This effect was abrogated in MDSCs treated with a PNT inhibitor. In a mouse model of tumor-associated inflammation in which the antitumor effects of antigen-specific CTLs are eradicated by expression of IL-1β in the tumor cells, we determined that therapeutic failure was not caused by more profound suppression of CTLs by IL-1β–expressing tumors than tumors not expressing this proinflammatory cytokine. Rather, therapeutic failure was a result of the presence of PNT. Clinical relevance for these data was suggested by the observation that myeloid cells were the predominant source of PNT in human lung, pancreatic, and breast cancer samples. Our data therefore suggest what we believe […]

Tumor-infiltrating myeloid cells induce tumor cell resistance to cytotoxic T cells in mice

Tangying Lu,[1] Rupal Ramakrishnan,[1] Soner Altiok,[2] Je-In Youn,[1] Pingyan Cheng,[1] Esteban Celis,[1] Vladimir Pisarev,[3,4] Simon Sherman,[3] Michael B. Sporn,[5] and Dmitry Gabrilovich[1]

[1]Department of Immunology and [2]Department of Pathology, H. Lee Moffitt Cancer Center, Tampa, Florida, USA. [3]University of Nebraska Medical Center, Omaha, Nebraska, USA. [4]Research Center for Medical Genetics, Moscow, Russia. [5]Dartmouth Medical School, Hanover, New Hampshire, USA.

Cancer immunotherapeutic approaches induce tumor-specific immune responses, in particular CTL responses, in many patients treated. However, such approaches are clinically beneficial to only a few patients. We set out to investigate one possible explanation for the failure of CTLs to eliminate tumors, specifically, the concept that this failure is not dependent on inhibition of T cell function. In a previous study, we found that in mice, myeloid-derived suppressor cells (MDSCs) are a source of the free radical peroxynitrite (PNT). Here, we show that pretreatment of mouse and human tumor cells with PNT or with MDSCs inhibits binding of processed peptides to tumor cell–associated MHC, and as a result, tumor cells become resistant to antigen-specific CTLs. This effect was abrogated in MDSCs treated with a PNT inhibitor. In a mouse model of tumor-associated inflammation in which the antitumor effects of antigen-specific CTLs are eradicated by expression of IL-1β in the tumor cells, we determined that therapeutic failure was not caused by more profound suppression of CTLs by IL-1β–expressing tumors than tumors not expressing this proinflammatory cytokine. Rather, therapeutic failure was a result of the presence of PNT. Clinical relevance for these data was suggested by the observation that myeloid cells were the predominant source of PNT in human lung, pancreatic, and breast cancer samples. Our data therefore suggest what we believe to be a novel mechanism of MDSC-mediated tumor cell resistance to CTLs.

Introduction

Historically, the main factor limiting the success of cancer immunotherapy was felt to be the inadequate tumor-specific immune responses generated in cancer patients. In recent years, however, advances in the development of novel methods of antigen delivery and the blockade of checkpoint proteins responsible for negative signaling in the immune system — as well as the generation of antigen-specific T cells ex vivo with subsequent transfer of these cells to patients after lymphoid depletion — have changed this situation. It is now possible to induce tumor-specific immune responses in most patients treated with various types of cancer immunotherapy (1–4). However, despite these successes, the proportion of patients who benefit clinically from these treatments remains small (5). Why has our ability to generate tumor-specific immune responses not translated into a clinical benefit? It is clear that the tumor microenvironment may provide protection of tumors even against potent CTL responses. One possible explanation could be an inhibition of CTLs at the tumor site via numerous mechanisms associated with tumor cells as well as with tumor-infiltrating myeloid and lymphoid cells (6). However, recent results of mouse experiments and clinical trials in patients with adoptive transfer of antigen-specific T cells suggested that this may not be entirely the case. Adoptive transfer of T cells is performed after lymphodepletion with either non-myeloablative chemotherapy or radiation. These treatments can reduce the presence of immune-suppressive factors in tumor-bearing hosts and enhance the immune responses to tumors (7, 8). This led us to ask what mechanisms could contribute to the inability of adoptively transferred CTLs to eliminate the tumors.

Inflammation plays an important role in the development and progression of different tumors. In the context of an inflammatory response, myeloid cells are the primary recruited effectors (9). In cancer, these cells are represented by activated macrophages, granulocytes, and myeloid-derived suppressor cells (MDSCs). In mice, MDSCs — which are morphologically, phenotypically, and functionally distinct from mature macrophages and granulocytes — are broadly characterized as $Gr\text{-}1^+CD11b^+$ and represent the predominant population of tumor-associated myeloid cells (10). Production of ROS and reactive nitrogen species (RNS) is one of the major characteristics of all activated myeloid cells. The production of most cellular ROS begins with the monovalent reduction of oxygen to the radical superoxide ($O_2^{\cdot-}$). One of the most common molecules that reacts with $O_2^{\cdot-}$ is NO, a key biological messenger in mammals. This leads to the formation of the free radical peroxynitrite (PNT) $ONOO^-$. Nitrosylation of tyrosine residues has been long recognized as a marker of PNT activity (11). In addition, PNT can react directly with cysteine, methionine, and tryptophan (11). A substantial number of studies have demonstrated high levels of nitrotyrosine (NT) in different types of cancer, including pancreatic cancer (12), malignant gliomas (13), head and neck cancer (14), mesothelioma (15), colon carcinoma (16), invasive breast carcinomas (17), melanoma (18, 19), and lung cancer (20). In patients with breast cancer, high tumor NT levels were associated with reduced disease-free and overall survival. In multivariate analysis, high NT levels emerged as a significant independent predictor for overall survival (17), and it was suggested that RNS were expressed not only in stromal cells and macrophages near tumor cells, but also in the tumor cells themselves (21). It is apparent that the levels of RNS in tumors varied, and in some studies increases in RNS were not observed (22).

The negative effect of ROS on T cell function in tumor-bearing mice is well described (23–27). We have demonstrated that MDSCs induced T cell tolerance via production of PNT and nitration/nitrosylation of TCRs and CD8 molecules on the surface of T cells.

Conflict of interest: The authors have declared that no conflict of interest exists.
Citation for this article: *J Clin Invest.* 2011;121(10):4015–4029. doi:10.1172/JCI45862.

TCRs lost the ability to recognize specific peptide/MHC (pMHC) complexes and perform their antitumor activity (28). This observation was consistent with reports in different experimental systems that conversion of a single tyrosine residue to NT can profoundly affect the recognition of MHC class II– and class I–restricted epitopes by $CD4^+$ and $CD8^+$ T cells, respectively (29, 30).

The fact that PNT can induce post-translational modifications of cell surface molecules without affecting cell viability suggested that it may play a much broader role in tumor escape from immune-mediated killing than inhibition of the T cell function. We consider that increased levels of PNT at the tumor site may cause post-translational modifications in tumor cells and render them resistant to CTLs. This would prevent tumor elimination even in a situation where potent CTL responses were generated. In this study we have tested this concept.

Results

Effect of PNT on tumor cell recognition by CTLs. To evaluate the effect of PNT on tumor cells, we used either the PNT donor 3-morpholinosydnonimine hydrochloride (SIN-1) or PNT. We selected the doses of the compounds that caused modest increases in the level of NT in tumor cells without substantial toxicity to EL-4 target cells. PNT at 0.1 mM caused less than 10% EL-4 cell death, with a clearly detectable increase in the NT level (Supplemental Figure 1; supplemental material available online with this article; doi:10.1172/JCI45862DS1). As effector cells we used OT-1 transgenic $CD8^+$ T cells recognizing the chicken OVA–derived peptide SIINFEKL in the context of $H\text{-}2K^b$. EL-4 target cells were treated with either SIN-1 or PNT for 10 minutes, washed, loaded with control or OVA-derived specific peptides, and then used in cytotoxicity assays. Pre-treatment of EL-4 cells with SIN-1 (Figure 1A) or PNT (Figure 1B) significantly ($P < 0.01$) reduced the ability of OT-1 CTLs to kill the OVA peptide–loaded targets as measured in a chromium release assay. To confirm these findings, we employed an additional cytotoxicity assay, which is based on the flow cytometric analysis of the proportion of specific target cells remaining in culture after incubation with CTLs. PNT significantly ($P < 0.05$) reduced the CTL killing of target cells loaded with specific (OVA) but not with a control irrelevant peptide (Figure 1C). The effect described above was observed only when the tumor cells were treated with SIN-1 or PNT prior to addition of specific peptide. If target cells were first loaded with the peptide and then treated with SIN-1 or PNT, the CTL-mediated killing was not affected (Figure 1, D–F). To assess the possible effect of PNT on CTL recognition of naturally processed antigens, we used EG-7 tumor cells (EL-4 cells transduced with OVA), which are recognized by OVA-specific OT-1 CTLs (Figure 1, G–I). SIN-1 and PNT treatment of EG-7 cells significantly ($P < 0.01$) reduced their susceptibility to be lysed by CTLs (Figure 1, G–I). To extend these findings to a different experimental system, we used B16-F10 melanoma cells and Pmel-1 transgenic $CD8^+$ T cells that recognize an $H\text{-}2D^b$–restricted epitope from the melanosomal antigen gp100 corresponding to amino acid positions 25–33 expressed in B16-F10 cells (31). Pre-treatment of B16-F10 target cells with PNT substantially reduced the ability of activated CTLs to kill tumor cells (Supplemental Figure 2).

The above-described results suggested that PNT might affect the binding of specific peptides to MHC class I on tumor cells. To directly test this hypothesis, EL-4 cells were treated with PNT, washed, and then loaded with $H\text{-}2K^b$–matching OVA-derived specific or control peptides followed by staining with an Ab recognizing the OVA-specific epitope in the context of $H\text{-}2K^b$. Pre-treatment of tumor cells with PNT substantially reduced the peptide binding and formation of the pMHC complex as measured by flow cytometry, whereas PNT had no effect on the pMHC complexes when tumor cells were treated with PNT after the peptide loading (Figure 2A). Treatment with PNT did not affect the expression of the $H\text{-}2K^b$ molecule on the tumor cells when applied either before or after loading with the peptide (Figure 2B). We also tested the effect of SIN-1 on binding of two distinct survivin-derived HLA-A2 peptide epitopes (32) to human T2 target cells. Pre-treatment of the T2 cells with SIN-1 significantly reduced binding of the both tested peptides (Figure 2C). Next, we evaluated whether direct NT modification of peptide epitope would reduce its binding capacity to MHC. The results showed that nitration of the tyrosine in position 3 of a peptide epitope derived from telomerase reverse transcriptase (TERT) significantly reduced its binding to HLA-A2 in T2 cells (Figure 2D), demonstrating that nitration of either the MHC molecule or the peptide epitope can affect binding. Thus, PNT alters binding of the peptides to the MHC class I on the surface of tumor cells by impacting on the formation of pMHC complexes, diminishing effective recognition of the tumor cells by CTLs. However, in natural circumstances the pMHC complexes are assembled intracellularly in the ER and subsequently are transported to the cell surface for presentation to CTLs. Our data indicated that PNT blocked recognition by CTLs of the naturally processed peptide in EG-7 and B16-F10 cells. However, our results with exogenous peptide pulsing indicate that PNT did not affect the already-made pMHC complexes. These observations suggest that PNT exerts its main effect in EG-7 and B16-F10 cells in the recognition of naturally processed antigen during the assembly of the pMHC complex. To test this hypothesis, we used Lewis lung carcinoma (LLC) and B16-F10 melanoma cells transfected with a single-chain $H\text{-}2K^b$-SIINFEKL construct. In these cells the $H\text{-}2K^b$-SIINFEKL pMHC complex is synthesized as a fusion protein that does not require antigen processing and epitope assembly (33). The cells were treated with PNT at different concentrations, and binding of the anti-pMHC Ab was evaluated. At a concentration of 0.3 mM, PNT caused more than a 10-fold increase in the level of NT staining of tumor cells (Figure 2, E and F). However, PNT treatment did not affect the pMHC expression on the cell surface (Figure 2, E and F). Moreover, treatment of LLC single-chain $H\text{-}2K^b$-SIINFEKL cells with PNT did not affect their killing by OVA-specific CTLs (Figure 2G). These data support the hypothesis that PNT affects the formation of pMHC complexes, preventing CTL killing of the tumor cells. In contrast, PNT did not affect the ability of NK cells to kill their targets (Supplemental Figure 3).

Myeloid cells are the principal producers of PNT in lung cancer and induce tumor cell resistance to CTLs. Next, we investigated what cells could release PNT into the tumor microenvironment. We evaluated tumor tissues from 15 patients with lung adenocarcinoma, 2 patients with large cell lung carcinoma, 8 patients with breast ductal carcinoma, and 13 patients with pancreatic ductal carcinoma. All subjects underwent surgical resection of the primary tumors between 2008 and 2010. Immunohistochemistry of NT staining was used as a marker of PNT production. Pancytokeratin AE1/AE3 and CD33 Abs were used to confirm the epithelial and myeloid origins of the cells, respectively. Typical staining examples are shown in Supplemental Figure 4. NT measurements in tumor and myeloid cells were scored on a 4-level scale (0 to 3): 0: no positive cells; 1: few slightly positive cells; 2: less than 50% positive cells;

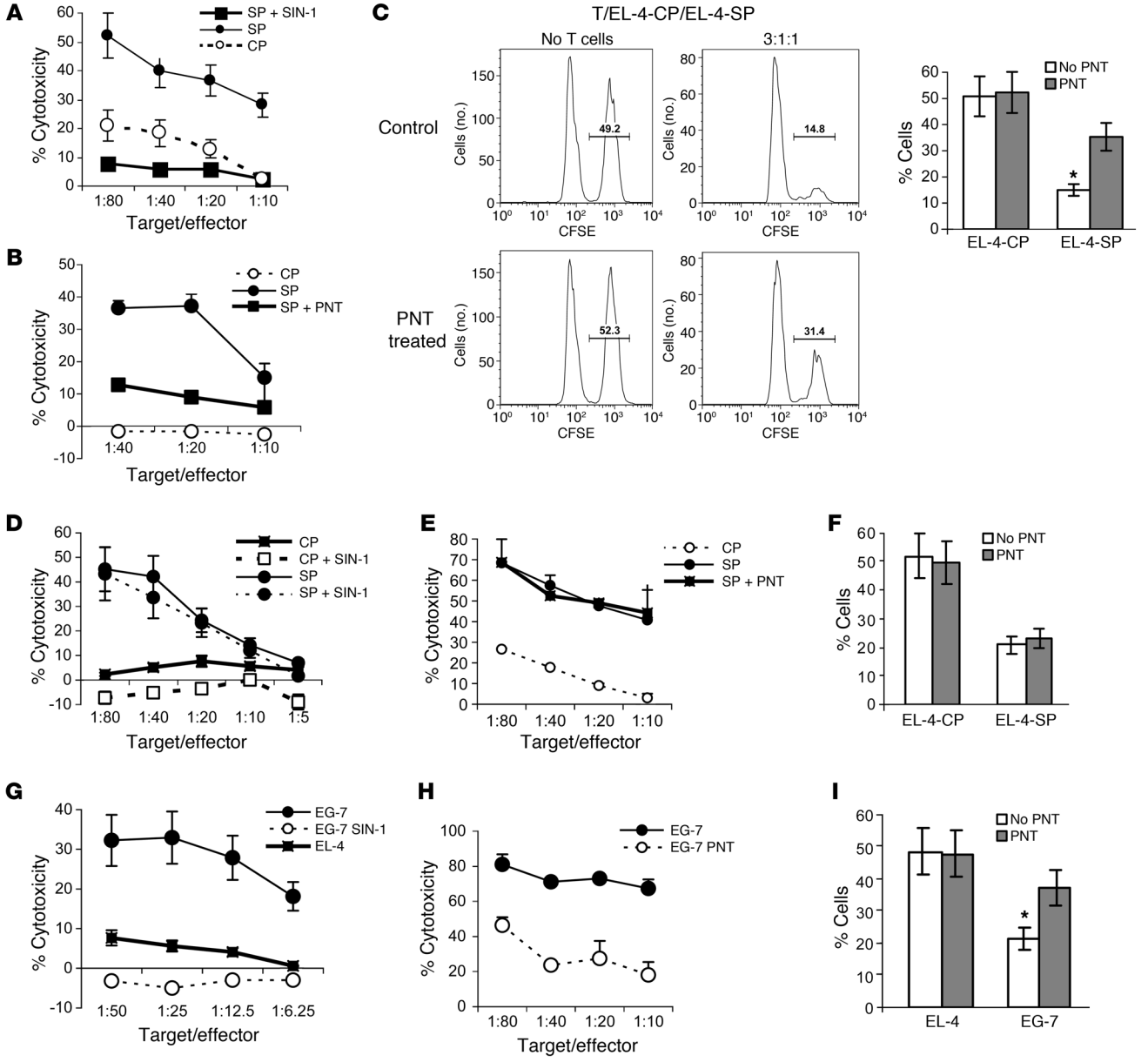

Figure 1

PNT makes tumor cells resistant to CTL-mediated lysis. (**A**) NO donor (1 hour pre-treatment with 1 mM SIN-1) inhibited killing of EL-4 cells subsequently washed and loaded with specific peptides (SP) by CTLs in chromium release assay. CP-EL-4 cells loaded with control peptide. (**B**) Pre-treatment of EL-4 cells with 0.1 mM PNT for 10 minutes inhibited killing of target cells by CTLs. In **A** and **B**, 3 experiments in duplicate were performed with similar results. Mean ± SEM of 1 experiment is shown. (**C**) Killing of EL-4 cells that were labeled with 2 doses of CFSE (high and low) and pre-treated with 0.1 mM PNT by CTLs. After washing EL-4 cells were loaded with a SP (high dose) or CP (low dose). Target cells were mixed at 1:1 ratio and were incubated with OT-1 T cells for 5 hours. Data are representative results of 3 experiments. Mean ± SEM of 3 experiments $^*P < 0.05$. (**D**–**F**) Experiments were performed as described in **A**–**C**, except that EL-4 target cells were first loaded with SP or CP and then treated with SIN-1 or PNT. (**D** and **E**) Three experiments in duplicate were performed, with similar results. Mean ± SEM of 1 experiment is shown. (**F**) Cumulative data (mean ± SEM) of 3 experiments are shown. (**G**–**I**) Experiments were performed essentially as described in **A**–**C**, except that EG-7 cells were used as targets instead of peptide-loaded EL-4 cells. (**G** and **H**) Three experiments in duplicate were performed, with similar results. Mean ± SEM of 1 experiment is shown. (**I**) Cumulative data (mean ± SEM) of 3 performed experiments are shown. $^*P < 0.01$.

3: almost all cells positive. In lung cancer patients, the rate of NT staining in myeloid cells (2.07 ± 0.21) was significantly higher than in tumor cells (0.58 ± 0.23, $P = 0.004$) or normal epithelial cells (0.76 ± 0.20, $P = 0.008$). Similar results were obtained in pancreatic cancer patients: myeloid cells (1.69 ± 0.21), tumor cells (0.15 ± 0.15, $P = 0.001$), epithelial cells (0.69 ± 0.20, $P = 0.02$). In breast cancer patients, the NT staining rate in myeloid cells was also higher than in tumor cells (2.25 ± 0.25 vs. 1.5 ± 0.38, $P = 0.06$). No difference was found in NT staining rates between myeloid and normal epithelial cells in breast cancer patients (2.1 ± 0.22, $P = 0.36$). Thus,

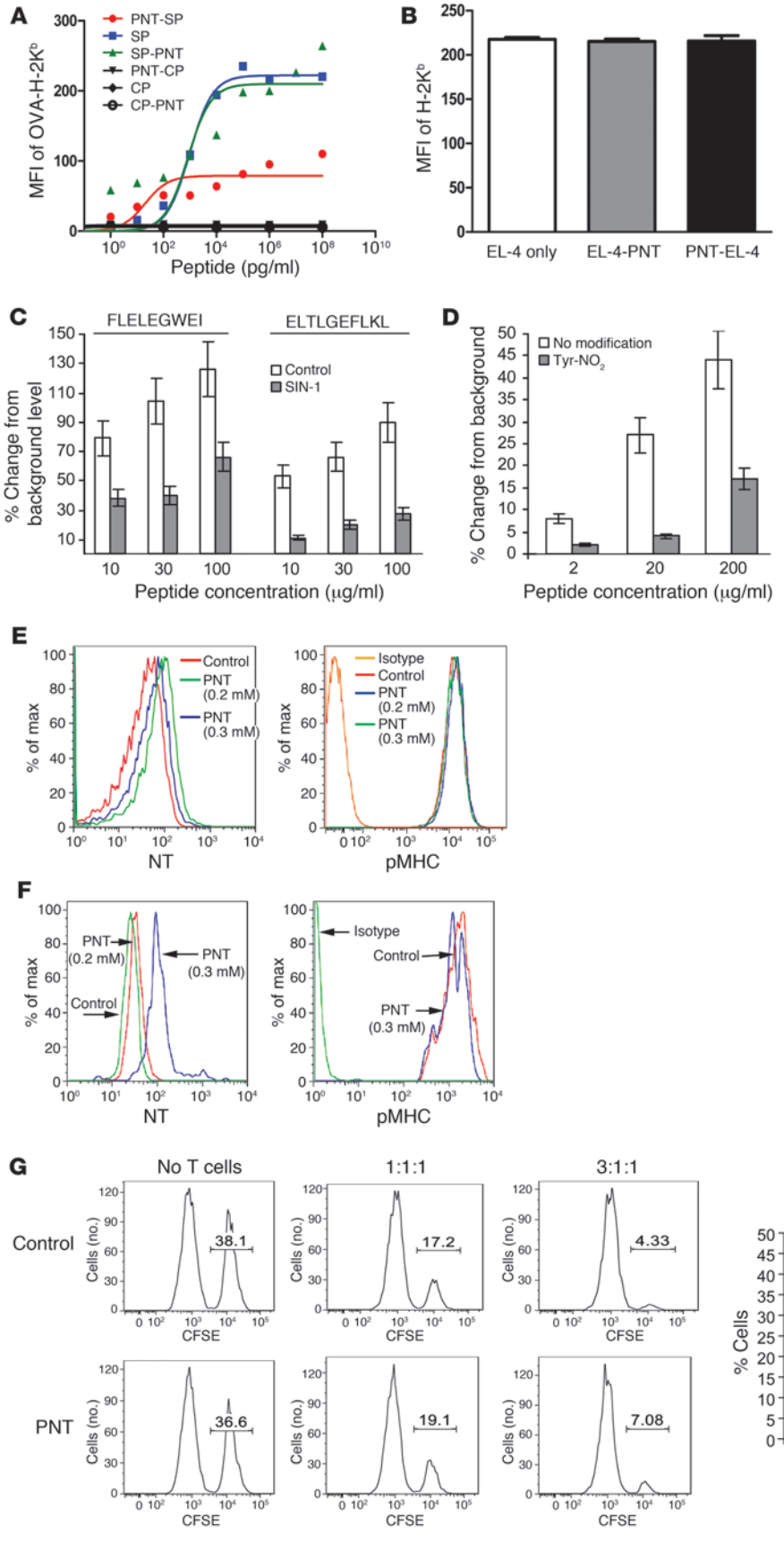

Figure 2

PNT affects binding of the peptides to MHC class I. (**A**) Pre-treatment of target cells with PNT decreased binding of the specific peptide. EL-4 cells were treated with 0.1 mM PNT before or after loading with specific or control peptides at the indicated concentrations. Specific peptide loaded on MHC class I was detected by florescence-conjugated anti-SIINFEKL bound to H-2K^b. Typical result of 1 of 5 performed experiments is shown. (**B**) Effect of PNT treatment on the expression of MHC class I (H-2K^b) molecules on EL-4 tumor cells. The MFI of H-2K^b expression is shown. Data represent mean ± SEM from 3 performed experiments. (**C**) Effect of pre-treatment of T2 human cells with SIN-1 on the binding of HLA-A2–matching human survivin-derived peptides. "Background" indicates T2 cells incubated without peptides. Mean ± SEM of 3 experiments is shown. $P < 0.05$, untreated versus SIN-1–treated cells for each experimental point. (**D**) Binding of non-modified HLA-A2–matched human TERT-derived PVYAETKHFL and nitrated PVY(NO$_2$)AETKHFL peptides to T2 cells. Mean ± SEM of 3 experiments is shown. $P < 0.05$, non-modified versus nitrated peptides for each experimental point. (**E** and **F**) PNT does not affect expression of pMHC on cells expressing single-chain H-2K^b-SIINFEKL protein. LLC (**E**) or B16-F10 (**F**) cells expressing single-chain H-2K^b-SIINFEKL were treated with PNT at indicated concentrations and then labeled with anti-NT or pMHC Abs. For each cell line, 2 experiments with the same results were performed. (**G**) PNT does not affect CTL killing of tumor cells expressing single-chain H-2K^b-SIINFEKL protein. Experiment was performed as described in **F**. LLC and LLC-H-2K^b-SIINFEKL cells were mixed at a 1:1 ratio and were untreated or pretreated with PNT, then used as targets for CTLs. Two experiments were performed, and cumulative results are shown.

myeloid cells were the predominant source of NT in lung, pancreatic, and breast cancer patients, while the normal ductal epithelial cells adjacent to breast cancer also showed moderate to strong NT positivity.

In LLC and EL-4 tumor tissues, practically all of the PNT production was associated with Gr-1$^+$ cells, which are primarily MDSCs, and to a lesser extent with F4/80$^+$ macrophages (Figure 3A). These results raised the question as to whether myeloid cells were able to cause tumor cell resistance to CTLs. Gr-1$^+$ MDSCs and F4/80$^+$ macrophages were isolated from spleens or tumor tissues of tumor-bearing mice and incubated with EL-4 tumor cells overnight. After that time, the myeloid cells were removed, and binding of the fluorescently labeled SIINFEKL peptide to the tumor cells was evaluated. Gr-1$^+$ immature myeloid cells (IMCs) from the spleen of naive mice did not affect peptide binding to the tumor cells, whereas MDSCs from spleen or tumor tissues had a significant inhibitory effect on the peptide binding to tumor cells (Figure 3B). The effect of macrophages on the peptide binding was much smaller and statistically not significant (Figure 3B). No effect of the myeloid cells on the expression of MHC class I on the surface of the tumor cells was detected (data not shown). To assess the ability of MDSCs to cause tumor cell resistance to CTLs, we preincubated EL-4 cells overnight with either MDSCs or control Gr-1$^+$ IMCs. Myeloid cells were then removed by bead purification, and the tumor cells were loaded with specific or control peptides and used as targets in a lysis CTL assay. Preincubation of tumor cells with MDSCs from spleens or tumors of EL-4 tumor–bearing mice did not affect the killing of EL-4 target cells loaded with control peptide but significantly reduced the killing of specific peptide–loaded target cells as compared with tumor cells preincubated with IMCs (Figure 3C).

To confirm that the PNT and MDSCs can indeed cause tyrosine nitrosylation of the MHC class I molecules in tumor cells, we cultured EL-4 cells with PNT and prepared whole cell lysates. H-2K^b molecules were immunoprecipitated, and membrane blots were probed with an anti-NT Ab. NT$^+$ staining was detected only in cells treated with PNT (Figure 3D). These results were further confirmed by confocal microscopy, where colocalization of MHC class I and NT was found on the tumor cells treated with PNT (Figure 3E). The expression of NT on tumor cells was also detected after overnight incubation with MDSCs but not with the control IMCs. Colocalization of NT with MHC class I was readily detectable (Figure 3F).

The fact that PNT produced by MDSCs caused modification of MHC molecules on tumor cells raised the question of why MDSCs themselves were able to present peptides to T cells and cause T cell tolerance (28, 34). It is known that neutrophils and macrophages have an elaborate system of antioxidants that protect them from excesses of ROS and RNS (35). To test this hypothesis directly, we treated EL-4 cells and MDSCs side-by-side with the same amount of PNT (0.1 mM). PNT did not affect the expression of MHC class I (H-2K^b) on EL-4 cells or MDSCs. However, it dramatically reduced binding of SIINFEKL peptide to EL-4 cells but not to MDSCs (Figure 4A).

PNT is a product of the interaction between NO and superoxide. To establish a causal relationship between the PNT production by MDSCs and their effect on tumor cells, we used two experimental approaches. First, MDSCs were generated from tumor-bearing mice lacking gp91^{phox}, a component of the NADPH complex responsible for the generation of ROS. MDSCs from these mice are not able to produce ROS in response to various stimuli (36). Second, we used the triterpenoid 2-cyano-3,12-dioxooleana-1,9(11)-dien-28-oic acid methyl ester (CDDO-Me; bardoxolone methyl). CDDO-Me is a compound that previously was demonstrated to inhibit ROS and PNT production by MDSCs (37). Both *gp91$^{phox-/-}$* MDSCs and MDSCs treated with CDDO-Me were unable to inhibit the peptide binding to MHC molecules by EL-4 tumor cells (Figure 4B). Treatment of tumor cells with CDDO-Me alone did not affect the peptide binding (Figure 4B). The CDDO-Me–treated MDSCs demonstrated significantly decreased protection of tumor cells from killing by CTLs (Figure 4C). To assess the possible effect of CDDO-Me in vivo, we established EL-4 tumors (CD45.2$^+$ cells) in congenic CD45.1$^+$ mice. The tumor-bearing mice (s.c. tumor diameter, 1.5 cm) were treated for 5 days with CDDO-Me, CD45.2$^+$ tumor cells were isolated, and specific peptide binding was measured. Short treatment with CDDO-Me did not substantially affect tumor size (data not shown) or expression of MHC class I on tumor cells (Figure 4D). However, tumor cells from mice treated with CDDO-Me had a substantially higher binding of the peptide than those from control untreated mice (Figure 4E). We asked whether treatment of mice with CDDO-Me made tumor cells more susceptible to CTL killing. Two tumor models with defined antigens were used: EG-7 thymoma, recognized by OT-1 CTLs, and B16-F10 melanoma recognized by gp100-specific Pmel-1 CTLs. Mice with established s.c. tumors were treated with CDDO-Me for 5 days, followed by tumor resection. Tumor cells were then used as targets in CTL assays. CDDO-Me treatment did not affect expression of MHC class I on tumor cells (Figure 5A). However, it enhanced CTL-mediated killing of both EG-7 (Figure 5, B and D) and B16-F10 (Figure 5, C and D) tumors. Thus, MDSCs generated in tumor-bearing mice produce large amounts of PNT, which affects the binding of the peptides to MHC class I on tumor cells, resulting in a decreased sensitivity of the tumor cells to CTL lysis.

Inflammation and tumor cell resistance to CTLs. To assess the biological significance of these findings, we modeled enhanced inflammatory conditions in vivo using the secreted proinflammatory cytokine IL-1β. We established several LLC cell lines: cells expressing OVA (LLC-OVA), cells expressing the secreted form of IL-1β (LLC-IL-1β), and cells expressing both OVA and IL-1β (LLC-IL-1β-OVA). Production of IL-1β was verified by ELISA of tumor cell supernatants. The IL-1β–transfected cell lines produced 200–300 pg/ml/24 hours, whereas in untransfected cells the IL-1β production was below the detectable level (Supplemental Figure 5A). Overexpression of OVA or IL-1β did not affect proliferation of tumor cells (Supplemental Figure 5B) or their ability to form colonies in semisolid medium (Supplemental Figure 5C). The expression of IL-1β by LLC-OVA cells did not affect their killing in vitro by OVA-specific CTLs (Supplemental Figure 6). However, the IL-1β–producing LLC cells grew faster than control LLC cells after s.c. injection into syngeneic C57BL/6 mice (Supplemental Figure 7). Therefore, we adjusted the concentration of tumor cells to provide for a comparable rate of tumor growth between the parental and IL-1β–producing LLC cells. Even when it was adjusted to achieve an equal tumor size, the IL-1β–producing tumors induced a much higher number of MDSCs in spleens and in tumor tissues than their parental cells (Figure 6A). Although expansion of macrophages was observed in the spleen, no differences in the proportion of tumor-associated macrophages was seen between the LLC-OVA and LLC-IL-1β-OVA tumor–bearing mice (Figure 6B). MDSCs generated in mice bearing LLC-OVA and LLC-IL-1β-OVA

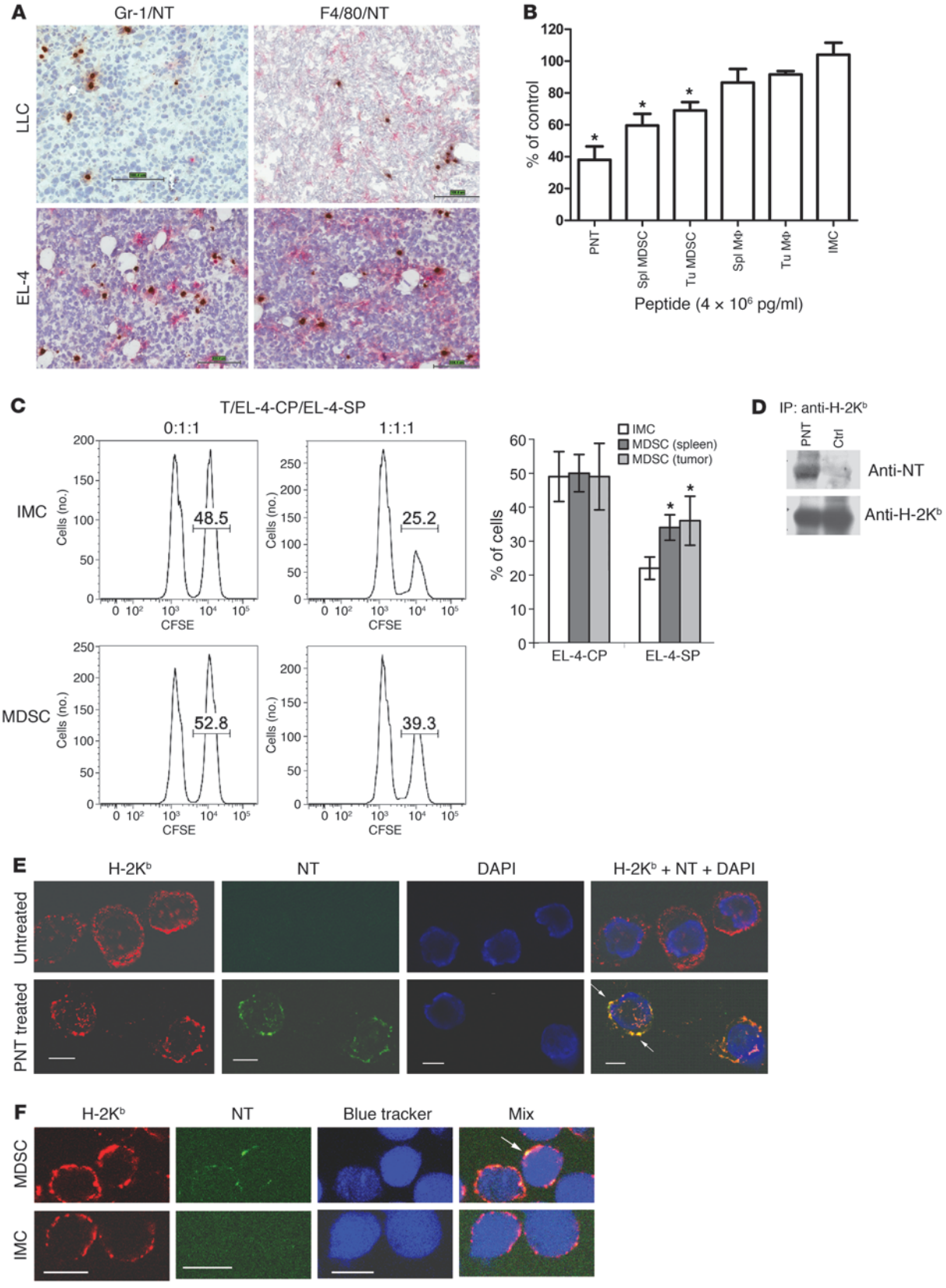
A
Gr-1/NT
F4/80/NT
LLC
EL-4
B
% of control
PNT
Spl MDSC
Tu MDSC
Spl MΦ
Tu MΦ
IMC
Peptide (4 × 10⁶ pg/ml)
C
T/EL-4-CP/EL-4-SP
0:1:1
1:1:1
IMC
MDSC
Cells (no.)
CFSE
48.5
25.2
52.8
39.3
IMC
MDSC (spleen)
MDSC (tumor)
% of cells
EL-4-CP
EL-4-SP
D
IP: anti-H-2Kᵇ
PNT
Ctrl
Anti-NT
Anti-H-2Kᵇ
E
H-2Kᵇ
NT
DAPI
H-2Kᵇ + NT + DAPI
Untreated
PNT treated
F
H-2Kᵇ
NT
Blue tracker
Mix
MDSC
IMC

Figure 3
MDSCs caused tumor cell resistance to CTLs. (**A**) NT (brown) and Gr-1+ or F4/80+ (red) staining in LLC and EL-4 tumors. Scale bars: 100 μm. (**B**) MDSCs reduced MHC class I binding ability to specific peptide (4 μg/ml) of EL-4 cells after overnight culture at a 1:1 ratio with indicated myeloid cells. Different concentrations of peptide were tested and showed similar results. PNT was used as a positive control. Percentage of change from MFI in untreated EL-4 cells set as 100% is shown. Spl, spleen; Tu, tumor; IMC, IMCs from the spleen of naive mice. Data are mean ± SEM from 4 experiments. $^*P < 0.05$ versus control. (**C**) MDSCs inhibit CTL killing of target tumor cells after overnight incubation. Myeloid cells were removed, and then EL-4 cells were used as targets in CTL assay as described in Figure 1C. Result of 1 typical experiment and cumulative data (mean ± SEM) of 3 performed experiments are shown. $^*P < 0.05$ versus IMC. (**D**) PNT caused nitration of tyrosine in MHC class I molecule (H-2Kb) in tumor cells. Immunoprecipitation of whole cell lysates from EL-4 cells treated with PNT was performed as described in Methods. Lysates precipitated with IgG showed no bands (not shown). (**E** and **F**) Colocalization of MHC class I and NT in tumor cells. (**E**) EL-4 cells treated with PNT and stained as indicated. (**F**) EL-4 cells were stained with blue trackers and cultured with MDSCs as described in **B**, myeloid cells were removed, and EL-4 cells were stained. Scale bars: 10 μm. Two experiments with the same results were performed.

tumors did not differ in the production of ROS (Figure 6C). The level of NO production was lower in MDSCs from the LLC-IL-1β-OVA mice than from the LLC-OVA mice (Figure 6D). However, large numbers of NT^+ MDSCs and macrophages were detected in the tumor tissues of the LLC-IL-1β-OVA–bearing mice (Figure 6, E and F, as compared with Figure 3A). Thus, overexpression of IL-1β in tumor cells resulted in the accumulation of a large number of PNT-producing MDSCs in tumor tissues.

We used these models to evaluate the effect of adoptive transfer of CTLs on the growth of tumors with induced inflammation. In preliminary experiments we determined the number of IL-1β–producing tumor cells that resulted in a rate of tumor growth similar to that of tumor cells with a low IL-1β level. The tumor cells were injected on day 0, and activated OVA-specific T cells were transferred to the mice on days 18 and 23 in this advanced model. As expected, transfer of the activated OVA-specific OT-1 T cells into the LLC-OVA tumor–bearing mice resulted in a significant ($P < 0.05$) delay in tumor progression compared with the LLC-bearing mice (Figure 6G). However, this effect was completely lost in the mice bearing tumors that produce IL-1β (Figure 6H).

It is now established that effective adoptive transfer therapy requires a lymphodepletion that can be achieved with chemotherapy or by total body irradiation (TBI) (38, 39). Therefore, we repeated experiments with the adoptive transfer of OVA-specific CTLs into tumor-bearing recipients treated with TBI followed by bone marrow transplantation. During the first 12 days after adoptive transfer, CTLs almost completely stopped the growth of LLC-OVA tumors, whereas in the control group tumors continued to grow. This resulted in almost 4-fold differences in tumor size between these two groups of mice (Figure 7A). However, this antitumor effect of CTLs was completely absent in the LLC-IL-1β-OVA tumor–bearing mice (Figure 7B). We investigated whether the observed effect was the result of profound immune suppression caused by the systemic expansion of MDSCs in mice bearing IL-1β–expressing tumors. We selected a time point (7 days after TBI and T cell transfer) when the antitumor effect in the LLC-OVA–bearing mice was apparent and in the LLC-IL-1β-OVA mice was absent (Figure 7, A and B). T cells were isolated from LN or tumor tissues and either restimulated with specific peptide–loaded naive antigen-presenting cells or exposed to anti-CD3/CD28 Abs. T cells from LLC-OVA and LLC-IL-1β-OVA tumor–bearing mice showed similar responses to both the specific antigen and nonspecific stimulation as measured in an IFN-γ ELISPOT assay (Figure 7C) or by T cell proliferation (Figure 7D).

We then measured levels of peripheral MDSCs and macrophages after TBI in these mice. Seven days after TBI, the numbers of MDSCs and macrophages in spleens of LLC-OVA– and LLC-IL-1β-OVA–bearing mice were dramatically and equally reduced to barely detectable levels (Figure 7, E and F). However, the number of MDSCs in LLC-IL-1β-OVA tumors was still significantly ($P < 0.05$) higher than in the LLC-OVA tumors (Figure 7E). Most importantly, the total number of PNT-producing myeloid cells in the tumor site was only marginally reduced 7 days after TBI (Figure 7G).

When T cell transfer to tumor-bearing mice was delayed by a week (to allow for partial reconstitution of the myeloid compartment after TBI), LLC-IL-1β-OVA tumors caused significantly stronger suppression than LLC-OVA tumors (Supplemental Figure 8).

We hypothesized that if MDSC-derived PNT was indeed responsible for the tumor cell resistance to CTLs, then the blockade of PNT with CDDO-Me would improve the effect of adoptive T cell therapy even in conditions of induced enhanced inflammation. Five-day treatment of mice bearing either LLC-OVA or LLC-IL-1β-OVA tumors with a CDDO-Me–containing diet caused a significant ($P < 0.05$) decrease in the number of NT^+ cells infiltrating the tumors (Figure 8A). We evaluated the antitumor effect of CDDO-Me on T cell therapy of tumor-bearing mice. LLC-OVA–bearing mice were treated with OVA-specific CTLs. In addition, the mice received 3 cycles of the CDDO-Me treatment (5 days each, with 3-day intervals, starting from day –2). CDDO-Me alone had only a moderate effect on tumor growth. In contrast, the addition of CDDO-Me to the T cell transfer resulted in a significant antitumor effect ($P = 0.01$) (Figure 8B). Experiments were stopped at that time, since mice in all control groups had to be sacrificed because tumor size in the control groups exceeded 2.5 cm in diameter (the maximum allowed by University of South Florida Health Sciences Center Animal Care and Use Committee regulations). Next, we evaluated the effect of CDDO-Me and T cells in LLC-IL-1β-OVA tumor–bearing mice. LLC-IL-1β-OVA–bearing mice were treated with TBI and OVA-specific CTLs. CDDO-Me alone had only a moderate effect on the growth of tumors. However, in contrast to the results described in Figure 7, the addition of CDDO-Me to the T cell transfer halted tumor progression for 4 weeks (Figure 8C) ($P = 0.018$). Since tumor cells expressing H-$2K^b$-SIINFEKL fusion protein (LLC-H-$2K^b$-SIINFEKL) were resistant to the negative effect of PNT (Figure 2, E–G), we asked whether this tumor would be more sensitive to T cell therapy than LLC-OVA. In contrast to the LLC-OVA tumor model, even in the absence of TBI or CDDO-Me treatment, OT-I T cells were able to completely reject LLC-H-$2K^b$-SIINFEKL tumors (Figure 8D). Although these results are striking, it is very difficult to formally exclude the possibility that the effect of the treatment was caused, at least partially, by the higher expression and stability of the peptide-MHC fusion protein in these cells than pMHC complexes assembled in LLC-OVA. OT-I T cells showed more potent killing of LLC-H-$2K^b$-SIINFEKL than LLC-OVA tumor cells (Figure 2G and Supplemental Figure 6).

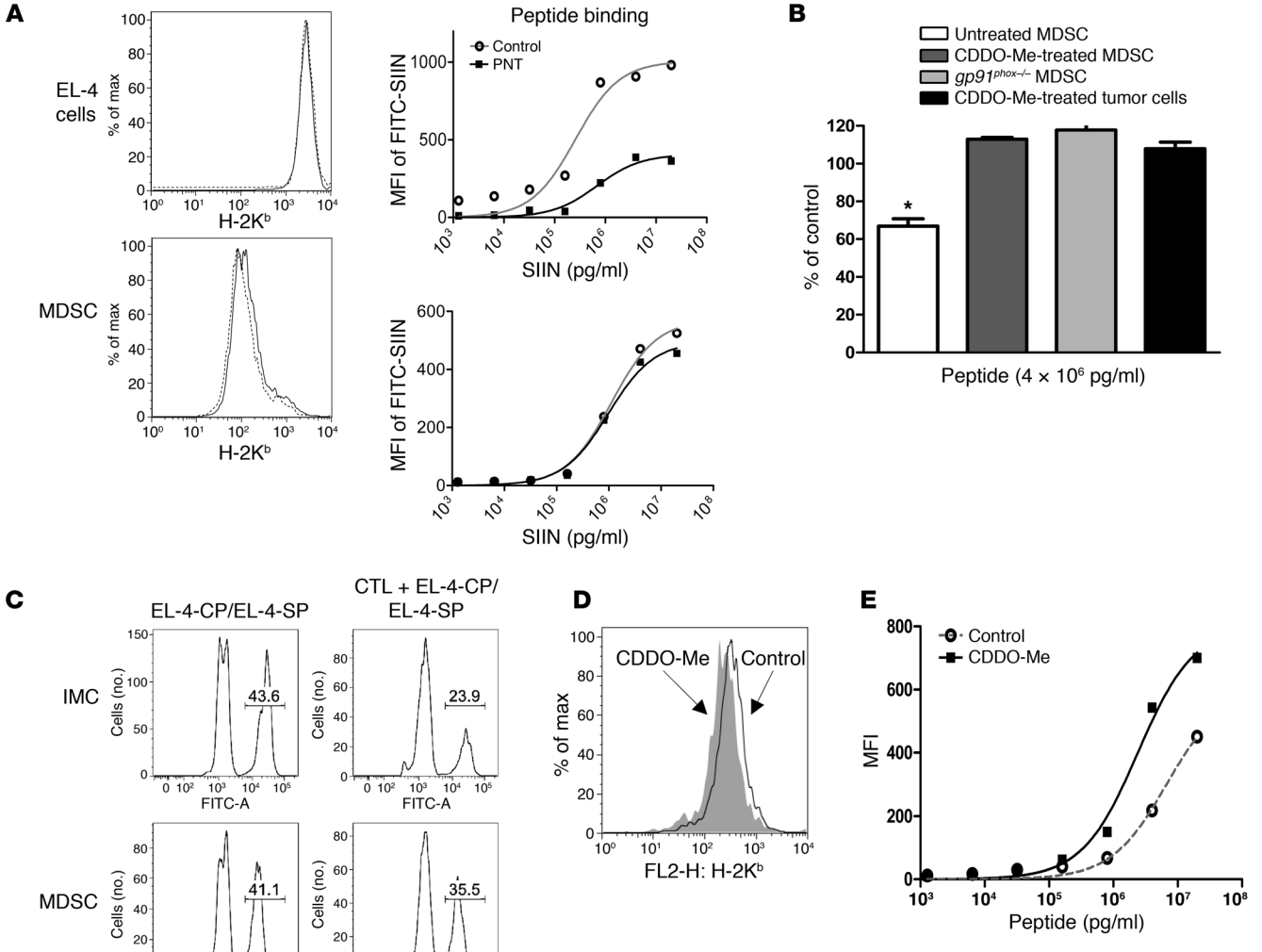

Figure 4

Effect of MDSCs on the protection of tumor cells from CTLs depends on ROS production. (**A**) MDSCs are resistant to PNT. MDSCs or EL-4 cells were treated for 10 minutes with 0.1 mM PNT. The levels of H-2Kb expression and NT after treatments were examined by flow cytometry (left panels). Cells were labeled with SIINFEKL peptide (SIIN) conjugated with FITC; peptide binding was performed by flow cytometry, and MFI was compared. Four experiments with similar results were performed. (**B**) Binding of FITC-SIINFEKL peptide was measured in EL-4 cells incubated with untreated MDSCs isolated from EL-4 tumor–bearing mice, in the presence of 250 nM CDDO-Me, or MDSCs isolated from EL-4 tumor–bearing *gp91$^{phox-/-}$* mice. As a control EL-4 cells were treated with CDDO-Me (250 nM). The background was set as 100% of peptide binding to untreated EL-4 cells. The graph shows the percentages of changes in MFI compared with background. Different concentrations of peptide were tested and showed similar results. One concentration, 4 μg/ml, is shown. Mean ± SEM of 4 experiments is shown. *$P < 0.05$ versus background. (**C**) EL-4 cells isolated from culture with MDSCs were loaded with control or specific peptides as target cells in CTL assays described in Figure 1C. MDSCs were from EL-4 tumor–bearing mice treated for 5 days with 150 mg/kg CDDO-Me or control diets. Representative 1 experiment and mean ± SEM of 3 performed experiments are shown. *$P < 0.05$ versus IMC-treated EL-4 cells. (**D** and **E**) Binding of peptides to tumor cells after treatment with CDDO-Me. EL-4 tumors were established in congenic (CD45.1$^+$) mice. Mice were treated with control or CDDO-Me diets for 5 days. EL-4 (CD45.2$^+$) cells were isolated by magnetic beads, and H-2K^b expression on tumor cells was examined by flow cytometry (**D**). Peptide binding was analyzed by incubation with FITC-SIINFEKL and evaluated by flow cytometry (**E**). Data are representative of 3 experiments with similar results.

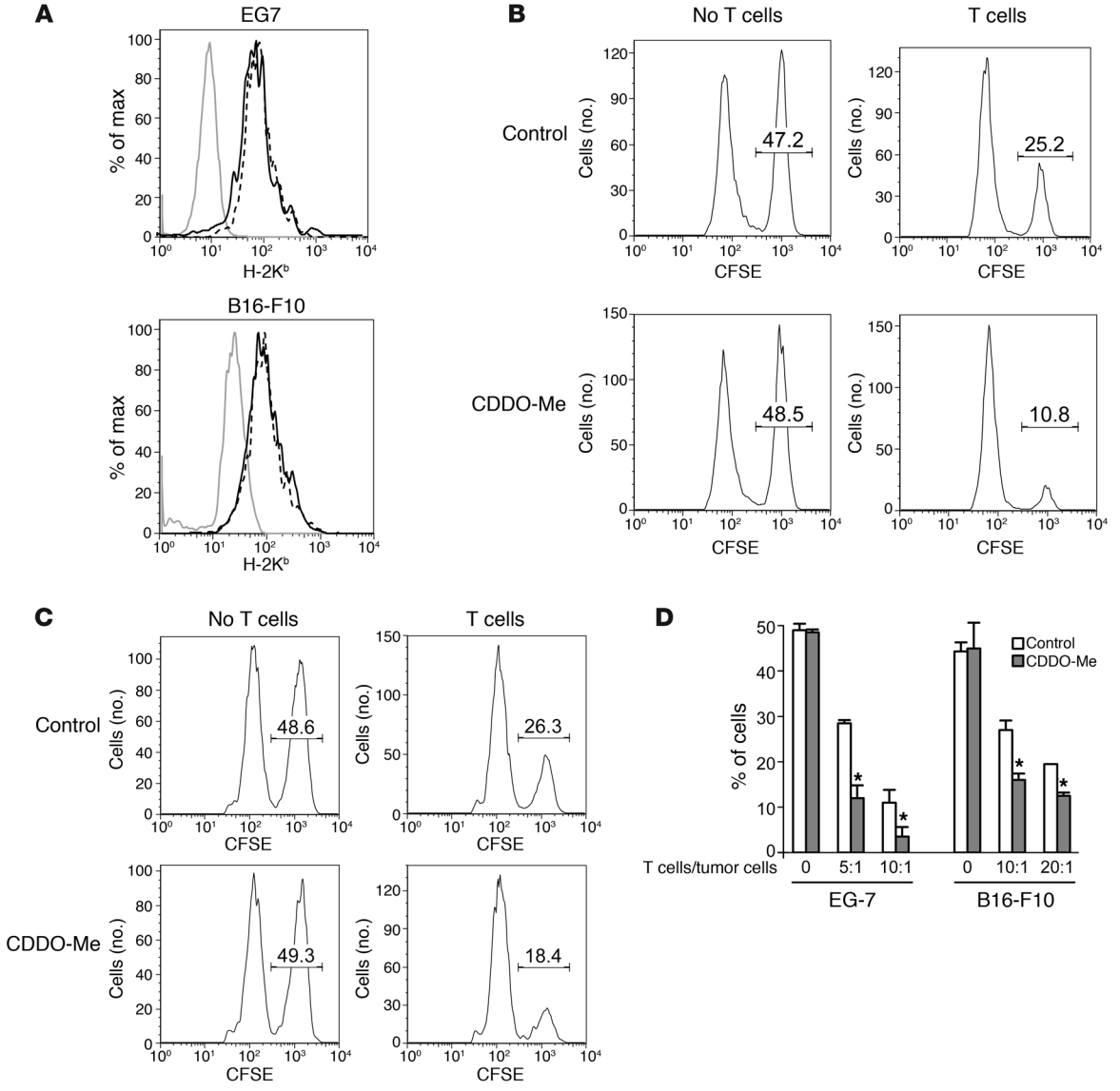

Figure 5

Effect of CDDO-Me treatment on CTL recognition of tumor cells. B16-F10 and EG-7 tumors were established s.c. in congenic (CD45.1$^+$) C57BL/6 mice. When tumors reached 1 cm in diameter, mice were treated with CDDO-Me diet for 5 days. B16-F10 tumor cells were isolated after collagen digestion and negative selection using anti-CD45 Abs and magnetic beads. EG-7 cells were isolated using anti-CD45.2 Ab and magnetic beads. Cells were then labeled with CFSE and used for CTL assay. (**A**) MHC class I (H-2K^b) expression in tumor cells isolated from nontreated (solid line) and CDDO-Me–treated (dotted line) mice. (**B**) CTL assay with tumor cells isolated from EG-7 tumor–bearing mice. Targets: EG-7 (high CFSE dose) and EL-4 (control, low CFSE dose); effector cells: OT-1 CTLs. (**C**) CTL assay with tumor cells isolated from B16-F10 tumor–bearing mice. Targets: B16-F10 (high CFSE dose) and LLC (control, low CFSE dose); effectors cells: pmel-1 CTLs. (**D**) Cumulative results of the experiments. Mean ± SD is shown. Each group included 2–3 mice. *$P < 0.05$.

To formally assess the role of CDDO-Me in increased tumor cell sensitivity to T cell therapy, we used H-2K^{b-} B16-F10 melanoma cells (40) and OT-1 CTLs that recognize irrelevant OVA-derived peptide. Adoptive transfer of Pmel-1 T cells slowed the growth of wild-type B16-F10 melanoma, and CDDO-Me significantly ($P = 0.04$) enhanced this effect (Figure 8E). As expected, no effect of OT-1 T cell transfer was observed in mice bearing H-2K^{b-} melanoma. CDDO-Me had effect on tumor growth. However, the combination of OT-1 T cell transfer with CDDO-Me treatment did not enhance the effect of the therapy (Figure 8F).

Discussion

The results of this study suggest a novel concept regarding tumor escape in cancer associated with inflammation. We propose that the myeloid cells infiltrating tumor sites induce tumor cell resistance to CTLs by modifying the pMHC complexes on tumor cells. These modifications reduce the capacity of the tumor cells' MHC to bind antigenic peptides and subsequently be recognized by CTLs. Although different types of chemical modifications of MHC molecules that would reduce CTL tumor recognition are possible, we specifically focused on nitration/nitrosylation. This mechanism

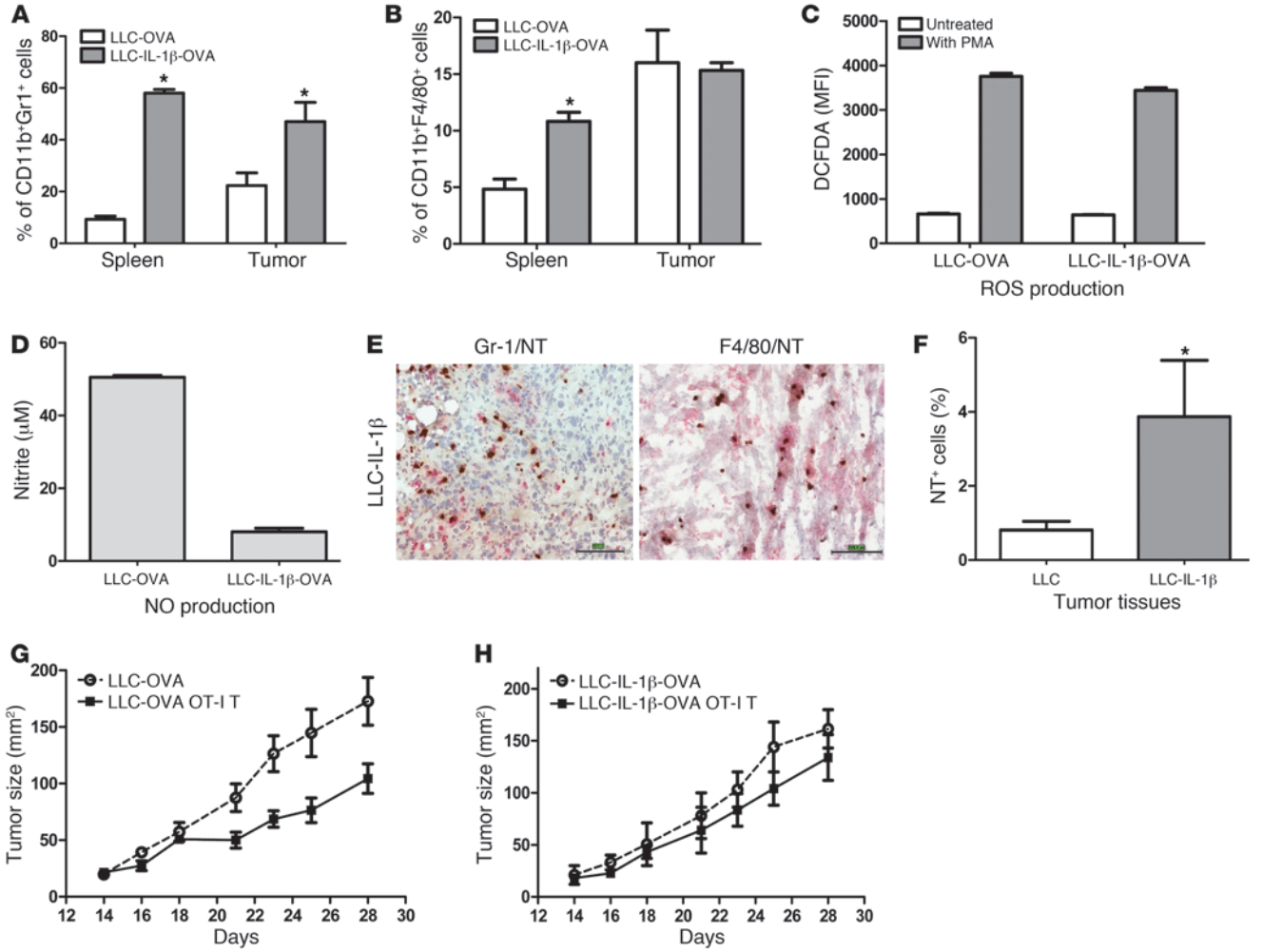

Figure 6

Experimental model of tumor-associated inflammation. (**A** and **B**) LLC-OVA or LLC-IL-1β-OVA tumors were established in C57BL/6 mice. The percentages of MDSCs (**A**) and macrophages (**B**) were determined in spleens and tumors by flow cytometry. Data are mean ± SEM for 3 experiments. *$P < 0.05$. (**C**) Measurement of ROS in splenic MDSCs using the oxidation-sensitive dye DCFDA. Cells were incubated with DCFDA (2 μM) with or without PMA (300 nM) for 30 minutes in serum-free media. Cells were then washed and detected by flow cytometry. Cumulative results of 3 experiments are shown. (**D**) NO production by MDSCs was measured by detection of nitrite concentrations. Cumulative results of 3 experiments are shown. (**E** and **F**) NT staining in LLC and LLC-IL-1β tumors. Double staining of NT^+ (brown) and either $Gr\text{-}1^+$ or $F4/80^+$ (red) cells in tumor tissues. Scale bars: 100 μm. (**E**) The percentages of NT^+ cells in LLC and LLC-IL1β tumor tissues analyzed by Aperio software. Ten fields (800 × 600 μm^2 each) were selected from each tumor, and mean ± SEM is shown. Four experiments with the same results were performed. *$P < 0.01$. (**G** and **H**) Antitumor effect of T cell therapy. Mice were injected s.c. with different numbers of LLC-OVA (**G**) or LLC-IL1β-OVA (**H**) cells, which provided for similar tumor sizes 2 weeks after inoculation. On days 18 and 23, 8×10^6 activated OT-I T cells were injected i.v. Tumors were measured. Each group included 9–12 mice. Data are mean ± SEM. In **G** the differences were significant on day 23. ($P < 0.05$).

is potentially important, since the myeloid cells are potent producers of ROS and RNS. NO and PNT, which are major components of this system, are extremely effective in causing nitrosylation of the 4 amino acids: tyrosine, tryptophan, cysteine, and methionine. Previous studies have demonstrated that the conversion of tyrosine residues to NT was sufficient to block the binding of peptide epitopes to MHC class I and class II (28–30). Here we confirmed this effect of PNT in tumor cells. More importantly, we addressed whether these observations bear biological relevance. Although it has been reported that tumor cells can produce RNS (21), in most tumors the main source of RNS and PNT is myeloid cells. Our data in human and mouse tumor tissues supported those observations. We have previously demonstrated that MDSCs in tumor-bearing mice are especially potent producers of ROS and PNT (36, 41). These cells together with mature macrophages are a major component of the inflammatory infiltrate in the tumor microenvironment. In our study, the preincubation of tumor cells with MDSCs induced the appearance of NT in tumor cells colocalized with MHC class I, correlating with reduced peptide epitope binding and decreasing the sensitivity of the tumor cells to CTLs. We concluded that MDSCs indeed were able to reproduce the effect of PNT on tumor cells. One question that arises was why the RNS-producing MDSCs did not kill tumor cells during coculture. It is known that the effect of NO on cells depends on the

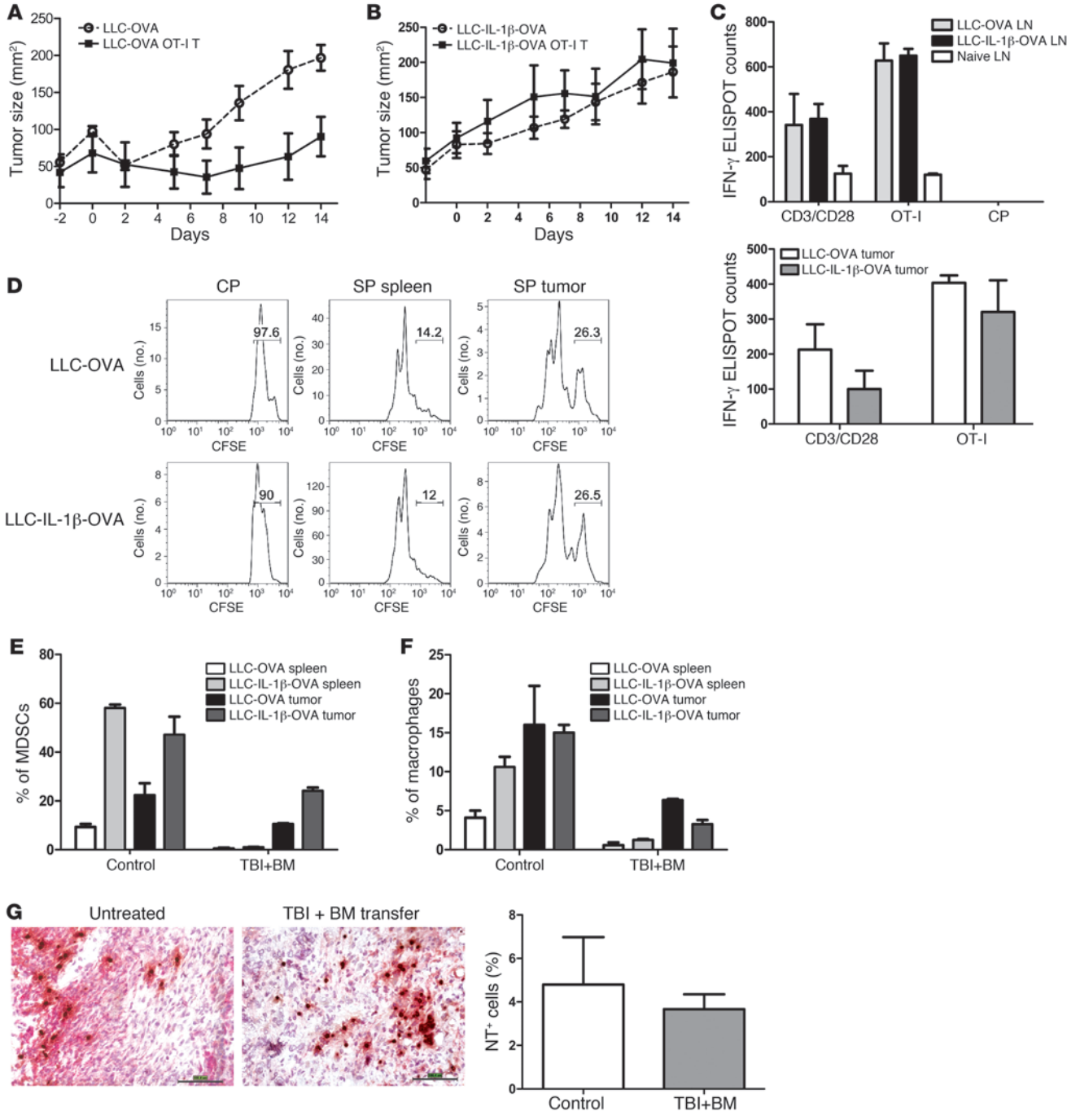

Figure 7

Inflammation reduced the effect of adoptive T cell therapy. (**A** and **B**) LLC-OVA (**A**) or LLC-IL-1β-OVA (**B**) tumors were established as described in Figure 6, G and H. All mice received TBI and bone marrow transplant on day 0. OT-I T cells were transferred to the treatment groups on day 1. Data are mean ± SEM. Each group included 9–12 mice. In **A** the differences were significant ($P < 0.01$). (**C** and **D**) T cell responses. Tumor-bearing mice received TBI with bone marrow transplant and T cell transfers as described in **A** and **B**. On day 7 T cells were isolated from LNs and tumors and mixed at a 1:1 ratio with irradiated syngenic control splenocytes and stimulated with either control or specific peptides, or anti-CD3/CD28 Abs. (**C**) IFN-γ production was measured in ELISPOT assays. The number of spots per 5×10^4 T cells was calculated. Each experiment was performed in triplicate and included 3 mice. Cumulative mean ± SEM is shown. (**D**) The proliferation of T cells isolated from spleens and tumors was determined by labeling of T cells with CFSE, followed by stimulation with specific or control peptides in the presence of irradiated naive splenocytes. The experiments were performed twice, with similar results. (**E** and **F**) The percentages of MDSCs (**E**) and macrophages (**F**) in spleen and tumor sites in mice 1 week after TBI and bone marrow transfer. (**G**) The number of NT⁺ cells in LLC-IL-1β-OVA tumors 7 days after TBI. Gr-1⁺ cells are red; NT⁺ cells are brown. Scale bars: 100 μm. Right panel: Cumulative results of the number of NT⁺ cells per 10 high-power fields (800×600 μm²). Each group included 3 mice.

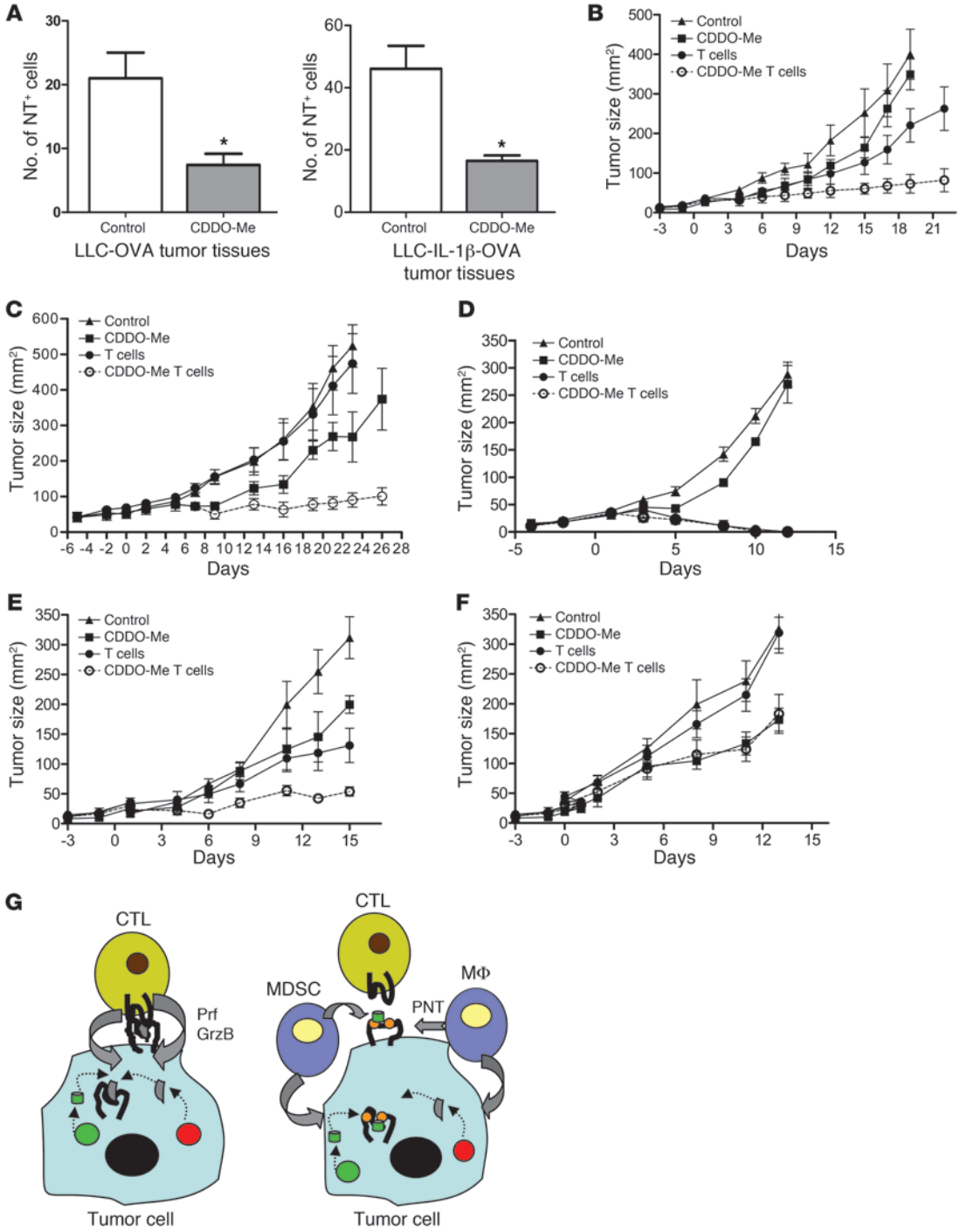

Figure 8

Inhibition of PNT production improves the antitumor effect of adoptive T cell transfer. (**A**) The number of NT+ cells per 10 high-power fields (800 × 600 mm²) in LLC-OVA and LLC-IL-1β-OVA tumors 5 days after treatment with 150 mg/kg CDDO-Me or control diets. Cumulative results of 3 mice per group.*$P < 0.05$. (**B**) Combined effect of CDDO-Me and T cell transfer on growth of LLC-OVA tumor. Tumor-bearing mice were treated with control and CDDO-Me diets for 5 days with 3 days interval started on day –2. OT-1 T cells were injected on days 1 and 8. Each group included 4–5 mice. The differences between CDDO-Me + OT-1 and other groups were significant ($P = 0.01$). (**C**) Combined effect of CDDO-Me and T cell transfer on growth of LLC-IL-1β-OVA tumor. All mice received TBI and bone marrow transfer on day 0. Each group included 4 mice. The differences between CDDO-Me + OT-1 and other groups were significant ($P < 0.05$). (**D**) Effect of T cell transfer on tumor growth of LLC-H-2K^b-SIINFEKL tumor. Each group included 4–5 mice. (**E** and **F**) Combined effect of CDDO-Me and T cell transfer on growth of B16-F10 (**E**) or H-2K^{b-} B16-F10 (**F**) tumors. Pmel-1 T cells were injected on days 1 and 8 into mice bearing B16-F10 melanoma (**E**) and OT-1 T cells to mice bearing H-2K^{b-} B16F-10 melanoma. Each group included 4–5 mice. The differences between CDDO-Me + T cells and other groups were significant ($P = 0.04$). In **E** but not in **F** ($P > 0.1$). (**B**–**F**) Mean ± SEM is shown. Tumor-bearing mice were treated as described in **B**. (**G**) Schematic of proposed effect of myeloid cells on tumor cell resistance to CTLs. Prf, perforin; GrzB, granzyme B. Red circles: processed antigen; brown: nitrated amino acids.

level of its production (42, 43). Apparently, the concentration of RNS released by MDSCs in these experiments was not sufficient to cause apoptosis of the tumor cells. This was consistent with the fact that infiltration of the tumors by myeloid cells does not result in elimination of tumor.

Our previous studies have shown that nitration of T cell receptors caused by MDSCs required close cell-to-cell contact between MDSCs and T cells. This contact was provided by the antigen-specific nature of the interaction (28). Such interaction does not take place between the tumor cells and MDSCs, which raises the question of the biologic relevance of this mechanism in tumor tissues. The initial answer comes from two recent studies of MDSCs and macrophages in tumor sites. We and others have demonstrated that NO production in tumor sites by MDSCs and macrophages was dramatically increased primarily via HIF-1α upregulation caused by hypoxia (44, 45). In tumor sites MDSCs do not require an antigen-specific interaction with T cells to cause inhibition of their activity (45). This suggested that the activated MDSCs and macrophages in the tumor site could affect neighboring tumor cells. To test this concept in vivo, we sought to establish tumors associated with an enhanced inflammatory response. IL-1β plays a major role in tumor-associated inflammation (46). Previous studies have demonstrated that overexpression of IL-1β in mammary carcinoma 4T1 resulted in substantially elevated levels of MDSCs. Neither T or B cells nor NKT cells were involved in the IL-1β–induced increase in MDSCs, since *Rag2*$^{-/-}$ and nude mice with 4T1/IL-1β tumors also have elevated MSDC levels (47). We generated several tumor cell lines by overexpressing the model antigen OVA and IL-1β in LLC tumor cells. IL-1β overexpression, as expected, resulted in a dramatic intratumoral accumulation of MDSCs and macrophages. Transfer of OVA-specific OT-1 CTLs was ineffective against IL-1β–producing tumors, despite the fact that tumor cells express OVA and were sensitive to killing in vitro. The most logical explanation that fits the existing model would be the existence of profound immune suppression caused by expanding MDSCs. In the 4T1 tumor model, this was exactly the case (47). However, in our experimental system we used TBI, which resulted in the elimination of MDSCs and macrophages from the spleen and a substantial reduction in these cells in the tumor sites. Our experiments showed that LN and tumor-associated T cells from LLC-OVA and LLC-OVA-IL-1β tumor–bearing mice responded to specific antigen equally, indicating that the inability of CTLs to block tumor growth in LLC-OVA-IL-1β mice was not due to more potent inhibition of T cell responses in these mice. These data are consistent with the concept that tumor-infiltrating MDSCs that remain after TBI retained PNT production and impacted the MHC molecules on tumor cells, which made them resistant to CTLs. Apparently, the remaining MDSCs were not sufficient to effectively inhibit the activated CTLs used for adoptive transfer. As expected, when more time was allowed for bone marrow reconstitution, LLC-IL-1β-OVA tumors caused more profound inhibition of T cell responses than LLC-OVA tumors.

An important role of PNT in the resistance of tumor cells to CTL lysis was further confirmed in experiments with CDDO-Me, a triterpenoid known to suppress the induction of iNOS in macrophages stimulated with various proinflammatory molecules, including IFN-γ, TNF-α, IL-1β, and lipopolysaccharide (48). CDDO-Me regulates a family of cytoprotective proteins that includes the enzymes of glutathione synthesis and transfer, thioredoxin, catalase, superoxide dismutase, and heme oxygenase (48–50). This results in a dramatic reduction in ROS and PNT in MDSCs (37). In our experiments CDDO-Me dramatically augmented the antitumor effect of adoptively transferred CTLs in the LLC-OVA-IL-1β tumor–bearing mice 7 days after the transfer. At that time the blockade of the antitumor effect of CTLs was not caused by inhibition of the T cell function, so it is likely that the impact of CDDO-Me was mediated by its direct effect on the tumor cells. This conclusion requires further validation in clinical settings. However, it suggests that inhibition of PNT can be a potentially valuable addition to the treatment of patients with bulky tumors undergoing adoptive T cell transfer therapy. Our data suggest a concept that may contribute to our understanding of the mechanisms of tumor immune escape. The tumor-infiltrating myeloid cells, particularly MDSCs, can induce nitration of MHC class I molecules on tumor cells, making them unable to effectively bind and retain peptides and thus rendering the tumor cells resistant to antigen-specific CTLs (Figure 8G). Under conditions of limited inflammation, tumor cells produce large numbers of peptides from different molecules. Tumor associated peptides are expressed as part of the pMHC complex on the surface of the cell. These peptides are identified as tumor-associated and used to generate CTLs. However, large numbers of activated myeloid cells, which are present in the inflammatory microenvironment, cause modifications of MHC class I that change their structure and thus the ability to bind specific peptides. Instead, other non-cognate peptides can bind to modified MHC class I groove. These peptides can be presented as part of pMHC on the surface. However, these peptides cannot be recognized by specific CTLs. This concept suggests that tumors could escape immune control even if potent CTL responses against the tumor-associated antigens were generated by vaccines, checkpoint inhibitors, or ex vivo expansion of tumor-infiltrating or genetically modified T cells. It also suggests that this escape can be diminished by blocking PNT production using pharmacological inhibitors of ROS or RNS.

Methods

Mice. C57BL/6 mice, 6–8 weeks of age, were obtained from the NIH. OT-1 TCR-transgenic mice and *gp91*$^{phox-/-}$ mice were purchased from The Jackson Laboratory. All animal procedures were approved by the University of South Florida Health Sciences Center Animal Care and Use Committee.

Cell lines. EL-4 and EG-7 thymomas, B16-F10 melanoma, and LLC were obtained from ATCC. Cells were cultured in DMEM (BioSource International) supplemented with 10% FBS, 5 mM glutamine, 25 mM HEPES, and 1% antibiotics (Mediatech). The LLC-IL-1β cell line was created by transfection of pLXSN/ssIL-1β plasmid, generated by R. Apte (Ben-Gurion University of the Negev, Beer-Sheva, Israel) and provided by S. Ostrand-Rosenberg (University of Maryland, College Park, Maryland, USA) using a Nucleofector kit (Amaxa, Lonza). Selection was performed using G418 (Calbiochem). Single-cell clones were evaluated for IL-1β production by testing with an hIL-1β ELISA kit (eBioscience). Chicken OVA cDNA was amplified by PCR using pAc-neo-OVA (provided by M.J. Bevan, University of Washington, Seattle, Washington, USA) as a template. The 5′ primer sequence was 5′-AACGCGGATCCACCATGGGCTCCATCGGCGC-3′, and the 3′ primer sequence was 5′-GAGCACCGCTCGAGTTTTTAAGGGGAAACACATC-3′. OVA expression plasmid was created by ligation of OVA cDNA into pcDNA3.1/Hygro(+) (Invitrogen) vector between BamHI and XhoI sites. To create LLC-OVA and LLC-IL1β-OVA cell lines, OVA plasmid was used to transfect LLC or LLC-IL1β cell lines and selected using hygromycin B (Invitrogen). OVA expression (45 kDa) in LLC-OVA and LLC-IL1β-OVA cell lines was confirmed by Western blotting (data not shown) using

anti-OVA mAbs obtained from Sigma-Aldrich. Transfected B16 and LLC cells expressing a single-chain H-2K^b-SIINFEKL protein were prepared as described previously (51) using a construct encoding a single-chain trimer H-2K^b-b2M-OVA$_{257-263}$ (33) molecule (provided by J. Connolly and T. Hansen, Washington University, St. Louis, Missouri, USA). After transfection, stable clones were isolated by a combination of drug selection, flow cytometry sorting with the H-2K^b-SIINFEKL–specific Ab 25.D1.16 (52), and cell cloning at limiting dilution.

Reagents, cell isolation, and treatment. DCFDA used for measurement of ROS production was obtained form Invitrogen. PNT and rabbit polyclonal anti-NT Ab were purchased from Upstate (Millipore). Abs against CD11b, Gr-1, F4/80, and isotype controls used in flow cytometry, cell isolation, and immunohistochemistry were obtained from BD Biosciences — Pharmingen. Gr-1$^+$ cells were isolated from spleens or tumors of tumor-bearing mice by magnetic beads and MiniMACS columns (Miltenyi Biotec). Prior to cell isolation, tumor tissues were cut into small pieces and treated with collagenase (type D, 1.4 g/l, Sigma-Aldrich) and DNase I (300 kU/l, Sigma-Aldrich) for 45 minutes at 37°C, and dead cells were removed by centrifugation over a Ficoll-Hypaque gradient (Atlanta Biotechnology). CDDO-Me was synthesized as described previously (53) and was administered to mice with chow (37).

Peptide-binding assay. EL-4 cells were treated with 0.1 mM PNT (10 minutes at room temperature, followed by 2 washes with PBS) either prior to or after loading with various concentrations of specific (H-2K^b, SIINFEKL) or control (H-2K^b, SIYRYYGL) peptides (American Peptides). Peptide binding was detected with FITC-conjugated Ab recognizing SIINFEKL bound to H-2K^b (eBioscience). Samples were evaluated by flow cytometry (LSR II, BD) and analyzed using the FlowJo (Tree Star) program. In other sets of experiments, EL-4 cells were cocultured with Gr-1$^+$ cells from tumor-bearing mice at a 1:1 ratio for 18 hours. Myeloid cells were removed by negative selection with anti–Gr-1 Abs and magnetic beads. EL-4 cells were then loaded with peptides and evaluated as described above.

Binding of survivin-derived and nitrated peptides was performed as described earlier (32) using tapasin-deficient T2 cells, intact or pulse-treated with 0.1 mM SIN-1 for 2 hours, followed by incubation with peptides for 16 hours. Binding of nitrated and control TERT-derived epitopes (PVY-AETKHFL and PVY[NO$_2$]AETKHFL) was similarly performed, except the nontreated T2 cells were used.

Tumor inoculation and adoptive cell transfer. C57BL/6 mice were injected s.c. with 5×10^5 tumor cells. In different tumor models, the optimal number of cells was selected to provide for a comparable rate of tumor growth. For the adoptive CTL treatment, OT-I or Pmel-1 T cells were activated in cultures with SIINFEKL peptide (5 μg/ml) for 2–3 days, and 8×10^6 T cells were injected i.v. at the indicated days. In some experiments mice were treated with 9.5 Gy myeloablative TBI, with bone marrow transfer (1.5×10^6 cells) 1 day before CTL adoptive transfer. Tumor size was measured with calipers every 2–3 days.

CTL assay. Target cells were labeled with CFSE (eBioscience) at a high dose (1 μM) and low dose (0.1 μM) or with 100 μCi chromium. When EL-4 cells were used as target cells, after different treatments EL-4 cells were incubated with specific (SIINFEKL) (high CFSE dose) or control (SIYRYYGL) (low CFSE dose) peptides at 1 μg/ml for 20–30 minutes. After washing, target cells were incubated with activated OT-1 T cells as effectors at the indicated ratios for 5 hours. Cells were then washed and analyzed by flow cytometry. EG-7 cells were treated with 100 ng/ml IFN-γ 48 hours prior to the experiments to enhance MHC class I expression.

Immunohistochemistry. Freshly isolated mouse tumor tissues were embedded in OCT medium in a plastic mold and frozen in dry ice. Sections cut from frozen blocks were dried for 1 hour at room temperature and fixed by acetone for 10 minutes. Sections were incubated with primary Abs or isotype controls diluted in blocking solution in a humidity chamber for 1 hour at room temperature or overnight at 4°C. After being washed 3–5 times in PBS, sections were incubated with secondary Ab for at least 45 minutes. VECTASTAIN ABC reagents were added on slides for 30 minutes at room temperature. Sections were then covered by AP or DAB substrates (Vector Laboratories) to develop the colors. The responses were stopped in 1–5 minutes, and slides were counterstained with Mayer's hematoxylin for 30 seconds and washed with tap water for 5–10 minutes. For double staining, the sections were blocked by Avidin-Biotin blocking reagents (Vector Laboratories) before the second staining process. Images were taken by the digital slide scanner Scanscope (Aperio) and analyzed by Aperio software.

Patient tumor sections from formalin-fixed and paraffin-embedded tissues were deparaffinized, and following antigen retrieval, tissue slides were stained with the mouse mAbs for Pan-cytokeratin (Spring Bioscience; 1:200 dilution), CD33 (Leica; 1:50 dilution), and NT (Millipore; 1:200 dilution) using the Ventana Discovery XT automated system (Ventana Medical Systems). Ventana Universal Secondary Antibody was used for 16 minutes at 37°C. The detection system used was the Ventana OmniMap detection kit, and slides were counterstained with hematoxylin. All washes were conducted with Ventana Reaction Buffer. Dehydration steps and coverslip procedure were completed manually as per the manufacturer's recommendations. Tissues were collected as part of H. Lee Moffitt Cancer Center tissue bank. Written informed consent was received from patients.

Confocal microscopy. EL-4 cells alone or pretreated with PNT were stained with Ab recognizing H-2K^b (BD Biosciences — Pharmingen) and after washing labeled with secondary Ab coupled to Texas red (Vector Laboratories) and anti-NT–Alexa Fluor 488 (Millipore). Cells were then cytospinned and mounted on slides with VECTASHIELD containing DAPI (Vector Laboratories). In another experiment, EL-4 cells pre-labeled with cell tracker blue CMAC (Molecular Probes) were cultured with splenic MDSCs (1:1 ratio) for 18 hours. Cells were then labeled with anti–H-2K^b and anti-NT Abs as indicated above. Cells were viewed on a Leica TCS SP5 confocal microscope with a ×63, 1.4 NA oil immersion objective.

Immunoprecipitation and immunoblotting. Tumor cell whole cell lysates were immunoprecipitated with purified anti-mouse H-2K^b Ab (BD Biosciences — Pharmingen) and TrueBlot Anti-Mouse Ig IP Beads (eBioscience). Immunoprecipitated proteins were separated by 10% SDS-PAGE, transferred to PVDF membrane, and treated with anti-NT Ab followed by HRP-conjugated secondary Ab. After detection, the membranes were stripped from the Ab and re-probed with Ab to anti-H-2K^b.

IFN-γ ELISPOT. MultiScreen-IP opaque 96-well plates (Millipore) were pre-wet with 70% methanol and coated overnight with purified anti–IFN-γ mAb (BD, Invitrogen). The plates were then blocked with 200 μl/well RPMI culture medium for 1–3 hours. Harvested T cells (50,000/well) were mixed with irradiated splenocytes from naive mice at a 1:1 ratio. The simulators were anti-CD3/CD28 (1 μg/ml each), OT-I–specific peptide SIINFEKEL (0.5 μg/ml), or control peptides (SIYRYYGL). The plates were incubated for 2 days. Biotinylated anti–IFN-γ Ab (BD Biosciences — Pharmingen) was added, and the plates were incubated overnight at 4°C, followed by 1 hour incubation with avidin–alkaline phosphatase. The plates were washed 4–6 times between steps. Spots were visualized by adding 100 μl/well of BCIP/NBT. Plates were scanned and counted using the ImmunoSpot analyzer (Cellular Technology).

Statistics. Statistical analysis was performed using a 2-tailed Student's *t* test and GraphPad Prism 5 software (GraphPad Software Inc.), with significance determined at $P < 0.05$. Tumor measurements were analyzed using 2-way ANOVA test with Bonferroni post-test.

Acknowledgments

This work was supported by American Recovery and Reinvestment Act supplement to NIH grant CA084488 to D.I. Gabrilovich

and by NIH grant CA136828 to E. Celis. We thank R. Apte and S. Ostrand-Rosenberg for the IL-1β construct; J. Connolly and T. Hansen for the single-chain H-2K^b/OVA construct; H-I Cho for making the cell lines; N. Fortenbery for NK cell isolations; and J. Weber for discussing and editing the manuscript. This work was partially supported by the flow cytometry and analytic microscopy cores at H. Lee Moffitt Cancer Center.

Received for publication April 26, 2011, and accepted in revised form July 27, 2011.

Address correspondence to: Dmitry Gabrilovich, H. Lee Moffitt Cancer Center, MRC 2067, 12902 Magnolia Dr., Tampa, Florida 33612, USA. Phone: 813.745.6863; Fax: 813.745.1328; E-mail: dmitry.gabrilovich@moffitt.org.

1. Jandus C, Speiser D, Romero P. Recent advances and hurdles in melanoma immunotherapy. *Pigment Cell Melanoma Res.* 2009;22(6):711–723.
2. Lasaro MO, Ertl HC. Targeting inhibitory pathways in cancer immunotherapy. *Curr Opin Immunol.* 2010;22(3):385–390.
3. Sarnaik AA, Weber JS. Recent advances using anti-CTLA-4 for the treatment of melanoma. *Cancer J.* 2009;15(3):169–173.
4. Muranski P, Restifo NP. Adoptive immunotherapy of cancer using CD4(+) T cells. *Curr Opin Immunol.* 2009;21(2):200–208.
5. Rosenberg SA, Dudley ME. Adoptive cell therapy for the treatment of patients with metastatic melanoma. *Curr Opin Immunol.* 2009;21(2):233–240.
6. Gabrilovich DI, Hurwitz A, eds. *Tumor Induced Immune Suppression: Mechanisms and Therapeutic Reversal.* New York, New York, USA: Springer-Verlag; 2007.
7. Safwat A. The immunobiology of low-dose total-body irradiation: more questions than answers. *Radiat Res.* 2000;153(5 pt 1):599–604.
8. Paulos CM, et al. Toll-like receptors in tumor immunotherapy. *Clin Cancer Res.* 2007;13(18 pt 1):5280–5289.
9. Coussens LM, Werb Z. Inflammation and cancer. *Nature.* 2002;420(6917):860–867.
10. Gabrilovich DI, Nagaraj S. Myeloid-derived suppressor cells as regulators of the immune system. *Nat Rev Immunol.* 2009;9(3):162–174.
11. Alvarez B, Radi R. Peroxynitrite reactivity with amino acids and proteins. *Amino Acids.* 2003; 25(3–4):295–311.
12. Vickers SM, MacMillan-Crow LA, Green M, Ellis C, Thompson JA. Association of increased immunostaining for inducible nitric oxide synthase and nitrotyrosine with fibroblast growth factor transformation in pancreatic cancer. *Arch Surg.* 1999; 134(3):245–251.
13. Cobbs CS, Whisenhunt TR, Wesemann DR, Harkins LE, Van Meir EG, Samanta M. Inactivation of wild-type p53 protein function by reactive oxygen and nitrogen species in malignant glioma cells. *Cancer Res.* 2003;63(24):8670–8673.
14. Bentz BG, Haines GK 3rd, Radosevich JA. Increased protein nitrosylation in head and neck squamous cell carcinogenesis. *Head Neck.* 2000;22(1):64–70.
15. Kinnula VL, et al. Ultrastructural and chromosomal studies on manganese superoxide dismutase in malignant mesothelioma. *Am J Respir Cell Mol Biol.* 2004;31(2):147–153.
16. Kojima M, et al. Nitric oxide synthase expression and nitric oxide production in human colon carcinoma tissue. *J Surg Oncol.* 1999;70(4):222–229.
17. Nakamura Y, et al. Nitric oxide in breast cancer: induction of vascular endothelial growth factor-C and correlation with metastasis and poor prognosis. *Clin Cancer Res.* 2006;12(4):1201–1207.
18. Ekmekcioglu S, Ellerhorst J, Prieto V, Johnson M, Broemeling L, Grimm EA. Early detection and diagnosis tumor iNOS predicts poor survival for stage III melanoma patients. *Int J Cancer.* 2005;119(4):861–866.
19. Ahmed B, Van Den Oord JJ. Expression of the inducible isoform of nitric oxide synthase in pigment cell lesions of the skin. *Br J Dermatol.* 2000; 142(3):432–440.
20. Masri FA, et al. Abnormalities in nitric oxide and its derivatives in lung cancer. *Am J Respir Crit Care Med.* 2005;172(5):597–605.
21. Vakkala M, Kahlos K, Lakari E, Paakko P, Kinnula V, Soini Y. Inducible nitric oxide synthase expression, apoptosis, and angiogenesis in in situ and invasive breast carcinomas. *Clin Cancer Res.* 2000; 6(6):2408–2416.
22. Rotondo R, et al. Arginase 2 is expressed by human lung cancer, but it neither induces immune suppression, nor affects disease progression. *Int J Cancer.* 2008;123(5):1108–1116.
23. Kono K, et al. Hydrogen peroxide secreted by tumor-derived macrophages down-modulates signal-transducing zeta molecules and inhibits tumor-specific T cell-and natural killer cell-mediated cytotoxicity. *Eur J Immunol.* 1996;26(6):1308–1313.
24. Aoe T, Okamoto Y, Saito T. Activated macrophages induce structural abnormalities of the T cell receptor-CD3 complex. *J Exp Med.* 1995;181(5):1881–1886.
25. Otsuji M, Kimura Y, Aoe T, Okamoto Y, Saito T. Oxidative stress by tumor-derived macrophages suppresses the expression of CD3 zeta chain of T-cell receptor complex and antigen-specific T-cell responses. *Proc Natl Acad Sci U S A.* 1996;93(23):13119–13124.
26. Schmielau J, Finn OJ. Activated granulocytes and granulocyte-derived hydrogen peroxide are the underlying mechanism of suppression of T-cell function in advanced cancer patients. *Cancer Res.* 2001; 61(12):4756–4760.
27. Bronte V, et al. Boosting antitumor responses of T lymphocytes infiltrating human prostate cancers. *J Exp Med.* 2005;201(8):1257–1268.
28. Nagaraj S, et al. Altered recognition of antigen is a novel mechanism of CD8+ T cell tolerance in cancer *Nat Med.* 2007;13(7):828–835.
29. Birnboim HC, Lemay AM, Lam DK, Goldstein R, Webb JR. Cutting edge: MHC class II-restricted peptides containing the inflammation-associated marker 3-nitrotyrosine evade central tolerance and elicit a robust cell-mediated immune response. *J Immunol.* 2003;171(2):528–532.
30. Hardy LL, Wick DA, Webb JR. Conversion of tyrosine to the inflammation-associated analog 3′-nitrotyrosine at either TCR- or MHC-contact positions can profoundly affect recognition of the MHC class I-restricted epitope of lymphocytic choriomeningitis virus glycoprotein 33 by CD8 T cells. *J Immunol.* 2008;180(9):5956–5962.
31. Overwijk WW, et al. Tumor regression and autoimmunity after reversal of a functionally tolerant state of self-reactive CD8+ T cells. *J Exp Med.* 2003;198(4):569–580.
32. Pisarev V, Yu B, Salup R, Sherman S, Altieri DC, Gabrilovich DI. Full-length dominant-negative survivin for cancer immunotherapy. *Clin Cancer Res.* 2003;9(17):6523–6533.
33. Wang B, et al. A single peptide-MHC complex positively selects a diverse and specific CD8 T cell repertoire. *Science.* 2009;326(5954):871–874.
34. Kusmartsev S, Nagaraj S, Gabrilovich DI. Tumor-associated CD8+ T cell tolerance induced by bone marrow-derived immature myeloid cells. *J Immunol.* 2005;175(7):4583–4592.
35. Splettstoesser WD, Schuff-Werner P. Oxidative stress in phagocytes—"the enemy within". *Microsc Res Tech.* 2002;57(6):441–455.
36. Corzo CA, et al. Mechanism regulating reactive oxygen species in tumor-induced myeloid-derived suppressor cells. *J Immunol.* 2009;182(9):5693–5701.
37. Nagaraj S, et al. Anti-inflammatory triterpenoid blocks immune suppressive function of myeloid-derived suppressor cells and improves immune response in cancer. *Clin Cancer Res.* 2010; 16(6):1812–1823.
38. Dummer W, et al. T cell homeostatic proliferation elicits effective antitumor autoimmunity. *J Clin Invest.* 2002;110(2):185–192.
39. Wrzesinski C, et al. Increased intensity lymphodepletion enhances tumor treatment efficacy of adoptively transferred tumor-specific T cells. *J Immunother.* 2010;33(1):1–7.
40. Cho HI, Lee YR, Celis E. Interferon gamma limits the effectiveness of melanoma peptide vaccines. *Blood.* 2011;117(1):135–144.
41. Kusmartsev S, Nefedova Y, Yoder D, Gabrilovich DI. Antigen-specific inhibition of CD8+ T cell response by immature myeloid cells in cancer is mediated by reactive oxygen species. *J Immunol.* 2004; 172(2):989–999.
42. Lechner M, Lirk P, Rieder J. Inducible nitric oxide synthase (iNOS) in tumor biology: the two sides of the same coin. *Semin Cancer Biol.* 2005;15(4):277–289.
43. Bogdan C. Nitric oxide and the immune response. *Nat Immunol.* 2001;2(10):907–916.
44. Doedens AL, et al. Macrophage expression of hypoxia-inducible factor-1 alpha suppresses T-cell function and promotes tumor progression. *Cancer Res.* 2010;70(19):7465–7475.
45. Corzo CA, et al. HIF-1α regulates function and differentiation of myeloid-derived suppressor cells in the tumor microenvironment. *J Exp Med.* 2010; 207(11):2439–2453.
46. Apte RN, Voronov E. Is interleukin-1 a good or bad 'guy' in tumor immunobiology and immunotherapy? *Immunol Rev.* 2008;222:222–241.
47. Bunt SK, Sinha P, Clements VK, Leips J, Ostrand-Rosenberg S. Inflammation induces myeloid-derived suppressor cells that facilitate tumor progression. *J Immunol.* 2006;176(1):284–290.
48. Liby KT, Yore MM, Sporn MB. Triterpenoids and rexinoids as multifunctional agents for the prevention and treatment of cancer. *Nat Rev Cancer.* 2007; 7(5):357–369.
49. Dinkova-Kostova AT, et al. Extremely potent triterpenoid inducers of the phase 2 response: correlations of protection against oxidant and inflammatory stress. *Proc Natl Acad Sci U S A.* 2005;102(12):4584–4589.
50. Yates MS, et al. Potent protection against aflatoxin-induced tumorigenesis through induction of Nrf2-regulated pathways by the triterpenoid 1-[2-cyano-3-,12-dioxooleana-1,9(11)-dien-28-oyl]imidazole. *Cancer Res.* 2006;66(4):2488–2494.
51. Cho HI, Lee YR, Celis E. Interferon gamma limits the effectiveness of melanoma peptide vaccines. *Blood.* 2011;117(1):135–144.
52. Porgador A, Yewdell JW, Deng Y, Bennink JR, Germain RN. Localization, quantitation, and in situ detection of specific peptide-MHC class I complexes using a mAb. Immunity. *Immunity.* 1997;6(6):715.
53. Honda T, Rounds BV, Gribble GW, Suh N, Wang Y, Sporn MB. Design and synthesis of 2-cyano-3,12-dioxoolean-1,9-dien-28-oic acid, a novel and highly active inhibitor of nitric oxide production in mouse macrophages. *Bioorg Med Chem Lett.* 1998; 8(19):2711–2714.